Colloids and Surfaces B: Biointerfaces 158 (2017) 203–212

Contents lists available at ScienceDirect

Colloids and Surfaces B: Biointerfaces

journal homepage: www.elsevier.com/locate/colsurfb

Full Length Article

Comparative analysis of poly-glycolic acid-based hybrid polymer starter matrices for *in vitro* tissue engineering

Melanie Generali[a,1], Debora Kehl[a,1], Andrew K. Capulli[b], Kevin K. Parker[b], Simon P. Hoerstrup[a,c,d,2], Benedikt Weber[a,c,d,*,2]

[a] *Institute for Regenerative Medicine (IREM), Center for Therapy Development and Good Manufacturing Practice, University of Zurich, Zurich, Switzerland*
[b] *Disease Biophysics Group, Wyss Institute for Biologically Inspired Engineering, John A. Paulson School of Engineering and Applied Sciences, Harvard University, Cambridge, USA*
[c] *Center for Applied Biotechnology and Molecular Medicine (CABMM), University of Zurich, Zurich, Switzerland*
[d] *Zurich Center for Integrative Human Physiology (ZIHP), University of Zurich, Zurich, Switzerland*

ARTICLE INFO

Article history:
Received 4 April 2017
Received in revised form 23 June 2017
Accepted 28 June 2017
Available online 1 July 2017

Keywords:
Poly-glycolic acid
Poly-lactic acid
Poly-4-hydroxybutyrate
Poly–caprolactone
Polymers
Tissue engineering

ABSTRACT

Biodegradable scaffold matrixes form the basis of any *in vitro* tissue engineering approach by acting as a temporary matrix for cell proliferation and extracellular matrix deposition until the scaffold is replaced by neo-tissue. In this context several synthetic polymers have been investigated, however a concise systematic comparative analyses is missing. Therefore, the present study systematically compares three frequently used polymers for the *in vitro* engineering of extracellular matrix based on poly-glycolic acid (PGA) under static as well as dynamic conditions. Ultra-structural analysis was used to examine the polymers structure. For tissue engineering (TE) three human fibroblast cell lines were seeded on either PGA-poly-4-hydroxybutyrate (P4HB), PGA-poly-lactic acid (PLA) or PGA-poly–caprolactone (PCL) patches. These patches were analyzed after 21 days of culture qualitative by histology and quantitative by determining the amount of DNA, glycosaminoglycan and hydroxyproline. We found that PGA-P4HB and PGA-PLA scaffolds enhance tissue formation significantly higher than PGA-PCL scaffolds ($p < 0.05$). Polymer remnants were visualized by polarization microscopy. In addition, biomechanical properties of the tissue engineered patches were determined in comparison to native tissue. This study may allow future studies to specifically select certain polymer starter matrices aiming at specific tissue properties of the bioengineered constructs *in vitro*.

1. Introduction

During the last years, the interdisciplinary field of tissue engineering (TE) has emerged as a platform for the development of biological substitutes. The overall goal is the repair and/or regeneration of tissues or organs to resolve major health related concerns in humans. Multiple disciplines, such as cell biology, biomaterial research and biomedical engineering have contributed to the advances of tissue engineering technologies. Any tissue engineering approach is composed of three major components: (1) cells, (2) biocompatible scaffolds, and (3) suitable biochemical (*e.g.* growth factors) and physical (*e.g.* cyclic mechanical loading) stimuli supporting tissue formation *in vitro* and *in situ* [1]. While the engineered living substitute develops, the biocompatible scaffold should degrade without leaving remnants in the body, requiring a so-called biodegradable starter matrix (scaffold).

A variety of synthetic biodegradable polymers has been investigated as TE scaffold materials, though the main disadvantage of these materials is their lack of functional groups [2,3]. This results in limited capacity to combine with bioactive elements to reinforce their cell affinity [3]. In general, functional synthetic polymers have unsaturated bonds [4], or functional groups such as hydroxyl [5], carboxyl [6], and amide [7], through which functional biomaterials can be chemically modified by biomolecules to improve their bioactivity [5]. Nonetheless, synthetic polymers have been extensively used for TE, given their high durability, flexibility, and mechanical strength [8]. In addition, production conditions of synthetic

* Corresponding author at: Institute for Regenerative Medicine (IREM), University of Zurich, Moussonstrasse 13, 8091 Zurich, Switzerland.
E-mail addresses: melanie.generali@usz.ch (M. Generali), debora.kehl@usz.ch (D. Kehl), acapulli@seas.harvard.edu (A.K. Capulli), kkparker@g.harvard.edu (K.K. Parker), simon_philipp.hoerstrup@usz.ch (S.P. Hoerstrup), benedikt.weber@usz.ch (B. Weber).
[1] These authors contributed equally to the study.
[2] These senior authors contributed equally to the study.

http://dx.doi.org/10.1016/j.colsurfb.2017.06.046
0927-7765/

polymers can be tightly controlled, hence making mechanical and physical properties of the material predictable, reproducible and precisely defined [9]. These characteristics make synthetic polymers to an interesting raw material for scaffold fabrication [8–10].

In particular, poly-glycolic acid (PGA), poly-lactic acid (PLA), poly-hydroxy alkanoate (PHA), poly -caprolactone (PCL) and their deriving copolymers have generated substantial interest as scaffold materials for the *in vitro* TE of bone, cartilage, as well as cardiovascular tissues [11–14]. PGA is most commonly used because it degrades at predictable time point and into (generally) biocompatible components [8]. Besides, the high porosity of PGA meshes permits a good diffusion, neovascularization and cellular infiltration [15]. Unfortunately, PGA meshes are biodegraded rapidly within few weeks and can therefore not withstand mechanical forces exerted to the materials and guide the shape of the bioengineered construct over longer culturing periods [15,16]. As a result, hybrid polymers have been designed in order to combine the shape-memory and mechanical stability of slowly degrading polymers with the fast degrading properties of polymers, such as PGA [17]. For instance, combinations of PGA with polymers such as (poly-4-hydroxybutyrate) P4HB or PLA have been widely explored [8,13,14,18,19]. PLA is synthesized by polymerization of lactic acid and can be eliminated through the citric acid cycle [15]. Due to the chiral nature of PLA, several distinct forms are existing: poly-L-lactide (PLLA), poly-D-lactide (PDLA) and LD racemic (PDLLA), respectively [15]. PLA can easily be processed and its degradation rates and physical/mechanical characteristics are adjustable over a wide range by using different molecular weights and copolymers [19,20]. Also ε-caprolactone and copolymers have been studied intensely and are frequently investigated for biomedical applications [15]. Interestingly, PCL degrades very slowly *in-vivo via* enzymatic degradation and hydrolysis [21]. Unlike PGA and PCL, which are synthetized using chemical methods, P4HB is produced naturally by microorganisms making it more challenging to be synthesized [22]. After implantation into the body, P4HB degrades mainly by bulk hydrolysis producing 4HB, a normal component of the mammalian body [10].

In 1998, Shinoka et al. reported surgical implantation of tissue engineered vascular grafts (TEVGs) in lambs, in which scaffolds were constructed from autologous cells seeded onto PGA grafts [23]. Further studies have been conducted, for instance, by using PGA-poly-L-lactic acid (PLLA) scaffolds for microvessels in mice [24] or scaffolds composed of polyglycolide knitted fiber, and an L-lactide and ε-caprolactone copolymer sponge for TEVGs in a canine inferior vena cava model [25]. The hybrid polymeric scaffold fabricated from either PGA or PLA fiber-based mesh coated with a 50:50 copolymer of L-lactide and ε-caprolactone (PCLA/PGA or PCLA/PLA) are more elastic than the PGA scaffold [26]. This results in an improved compliance match between the vessel and the conduit and ultimately in better surgical handling characteristics [26]. For both heart valve and vascular tissue engineering the use of PGA meshes coated with P4HB, meaning the combination of the thermoplastic characteristic of P4HB and the high porosity of PGA meshes, has been investigated intensively with promising results *in vitro* and in preclinical studies [27–29]. In 2006, Mol et al. provided the first evidence of living, functional pulmonary arteries engineered from vascular cells seeded on PGA/P4HB scaffolds in a growing lamb model [13]. In contrast, PCL has been mainly investigated for biomedical applications in bone and cartilage repair, as surgical suture as well as for drug delivery systems, especially those with longer working lifetimes [12,15]. Son et al. showed that a PCL/poly(methyl methacrylate) (PMMA) scaffold was suitable for cell growth *in vitro* and for new bone formation *in vivo* [30]. This study suggested that PCL/PMMA blends can be used for biopolymer composite scaffolds in bone tissue engineering [30]. In general, all polyesters are biocompatible and have formed the bases of numerous FDA approved medical devices for clinical use [9,31].

However, in spite of their frequent use in biomedical research and therapeutic products, there is still a lack of systematic comparative analyses, such as qualitative and quantitative assays of tissue formation and biomechanics between different synthetic polymers. Therefore, the present study aims at a systematic, multimodal comparison of three frequently used polymers (PGA, PLA, PCL) integrated into a co-polymer solution with P4HB for the *in vitro* engineering of extracellular matrix under static as well as dynamic conditions. These data might allow for a specific selection of a certain polymer starter matrices aiming at specific tissue properties of bioengineered materials *in vitro*.

2. Material and methods

2.1. Isolation and culture of human umbilical cord fibroblasts

Human umbilical cords (n = 3) were collected after full-term births with informed consent according to the cantonal ethics commission of Zurich, Switzerland [KEK-ZH-2009-0095] and processed for isolation of venous fibroblasts according to established protocols [32]. Briefly, the umbilical cord vein was isolated surgically and small tissue pieces were cut out using a dissecting scissors. Tissue pieces were placed on a sterile petri dish and were left to adhere to the bottom for 20 min. Culture medium containing DMEM high glucose (Sigma-Aldrich, Switzerland), 10% fetal bovine serum (Biowest, USA) and an antibiotic/antimitotic solution (Sigma-Aldrich, Switzerland), was gently added and changed every third day. Tissue pieces were removed after first cellular outgrowth after approximately 1–2 weeks of incubation under humidified incubator conditions at 5% CO_2 at 37 °C. Three different fibroblast cell lines (named B014, B015 and B020) were isolated.

2.2. Phenotyping of human fibroblasts

Isolated human cells (n = 3) were characterized using immunofluorescence staining for common myofibroblast markers. Therefore, cells were cultured on 3.5 cm^2 cell culture dishes, fixed with 4% paraformaldehyde (Sigma-Aldrich, Switzerland), and incubated over night at 4 °C with the following primary antibodies: alpha smooth muscle actin (1A4, Abcam, United Kingdom), Vimentin (Vim 3B4, Abcam, United Kingdom), CD90 (EPR3133, Abcam, United Kingdom), CD31 (JC70A, Dako, USA), and Phalloidin (Life Technologie, Switzerland). The following secondary antibodies were used: anti mouse Alexa Flour 488 (Invitrogen, USA) and anti rabbit Alexa Flour 488 (Invitrogen, USA) and Dapi (Sigma-Aldrich, Switzerland). Cells were analyzed with a DM6000B fluorescence microscope (Leica, Germany). Image processing was performed using the Leica software (Leica, Germany).

2.3. Proliferation assay

Cellular proliferation was assessed by determining the number of total cells based on the absorbance of crystal violet when cultured on a 24-well plate for up to 7 days. In brief, every day cells were fixed with methanol (Sigma-Aldrich, Switzerland) for 10 min and stained with 0.1% crystal violet (Artechemis, Switzerland) for 5 min. The 24-well plates were washed and air-dried. Cells were solubilized with 2% Na-deoxycholat (Sigma-Aldrich, Switzerland) while being heated at 60 °C for 10 min. The absorbance was analyzed at 550 nm using a standard ELISA reader Synergy HT (Bio TEK, USA). To obtain quantitative information a standard curve with serial dilutions was performed.

2.4. Surface morphology of biomaterials

Samples were mounted on electron imagining stubs using carbon tape and subsequently sputter coated in 5 nm of Pt/Pd (Quorum Technologies, EMS 300TD, USA) to reduce fiber degradation during imaging. A field emitting electron microscope was used to image samples at 15 kV power (Zeiss, FESEM Ultra Plus) for clarity. For each sample, four regions of interest (ROI) measuring 1000 × 800 um were imaged from which five fibers per ROI were measured using Image J software (NIH, v1.48s, line tool) to determine the average fiber diameter of an ROI. For scaffold porosity, an additional four ROIs measuring 3000 × 2250 um were imaged. Each porosity ROI image was then automatically thresholded in Image J and porosity was defined as the percent area that was non-fiber (ie empty/porous space).

2.5. Tissue engineering

2.5.1. Scaffold fabrication

Patches were fabricated from non-woven polyglycolic acid (PGA) meshes (thickness 1.0 mm; specific gravity 70 mg/cm3; Cellon, Luxembourg) and coated with either 1% poly-4-hydroxybutyrate (P4HB; TEPHA, Inc., USA) or 1% Poly(L-lactide) (PLA, Carbion, USA) or 1% polycaprolactone (PCL, Carbion, USA) by dipping into a tetrahydrofuran solution (Sigma-Aldrich, Switzerland). After solvent evaporation and vacuum drying overnight, the scaffolds were placed into a 70% EtOH (Sigma-Aldrich, Switzerland) for 30 min to obtain sterility, followed by two washing cycles with PBS (Sigma-Aldrich, Switzerland). Thereafter, scaffolds were pre-incubated in DMEM culture medium previously described for 12–24 h to facilitate cell attachment.

2.5.2. Cell seeding

Human fibroblasts (n = 3) were seeded onto scaffolds using a density of $1.5*10^6$ cells/cm^2. Therefore, fibrinogen (Sigma-Aldrich, Switzerland) (10 mg/mL of active protein) and thrombin (Sigma-Aldrich, Switzerland) were prepared, used and titrated to an optimal clotting time of approximately 30 s by adapting the concentration of fibrinogen. The cells were resuspended in a fibrinogen-thrombin co-solution and subsequently seeded onto the sterile scaffolds. After static incubation of seeded constructs in DMEM (10% fetal bovine serum; penicillin/streptomycin and 0.9 mM of L-ascorbic acid-2-phosphate (Sigma-Aldrich, Switzerland)) for 7 days, they were kept either under static conditions or placed onto a shaker for additional mechanical stimulation *via* shear stress. The constructs were harvested after 21 days of culture and processed immediately for subsequent analyses.

2.6. Qualitative tissue analysis

For immunohistochemical analysis of TE patches (n = 3 per group), sections with 5 μm thickness derived from blocks of formalin-fixed, paraffin-embedded tissue were mounted on glass slides (SuperFrost Plus, Menzel Gläser,Germany), deparaffinized, rehydrated and stained with hematoxylin and eosin (H&E) or Masson Trichrome using standard histological techniques. All sections were analyzed using a Mirax Midi BF slide scanner (Zeiss, Germany) and processed using MIRAX viewer (Zeiss, Germany).

2.7. Quantitative tissue analysis

TE patches (n = 6 per group) were minced, lyophilized, and analyzed using biochemical assays for total deoxyribonucleic acid (DNA) content as an indicator for cell number, hydroxyproline (HYP) content as an indicator for collagen, as well as for glycosaminoglycan (GAG) content. All TE patches were digested in papain (Sigma-Aldrich, Switzerland) solution (300 μg/mL in PBS with 5 mM EDTA (Sigma-Aldrich, Switzerland)) and 5 mM cysteine (Sigma-Aldrich, Switzerland), at 65 °C for 16 h. For measuring the cellularity of the constructs, the DNA amount was quantified according to manufacturer's protocol (Life Technologies, Switzerland, No. P11496). The GAG content was determined using a modified version of the protocol described by Ref. [33], and a standard curve prepared from chondroitin sulfate from shark cartilage (Sigma-Aldrich, Switzerland). Hydroxyproline was determined with a modified version of the protocol provided by Ref. [34]. Remnants of the hybrid polymers matrices were visualized using polarization microscopy (Zeiss, Germany).

2.8. Biomechanics

After 0 (only for the unseeded group) and 21 days of culture, the mechanical properties of the TE constructs (n = 4 per group) were assessed using a uniaxial tensile tester (Instron 5864, Boston, MA, USA) equipped with a 100-N load cell. For comparison, native tissues (cartilage, skin and vein) were harvested from sheep post mortem provided by the local slaughterhouse Zurich/Hinwil, Switzerland (n = 4). The crosshead speed was set to correspond to an initial strain rate of 7 mm/min and the tester operated at 5 bars of air pressure. Patches had a cross-sectional area of 14 mm × 4 mm × 1 mm (length × width × thickness) and were fixed with hydraulic clamps. Stress–strain curves were obtained and Young's modulus was determined as the slope of the curve at a strain of 10%, as a measure for tissue stiffness.

2.9. Statistic

Quantitative data are presented as mean ± standard deviation. For statistical comparison of the proliferation rate of the three different cell lines a one-way ANOVA was performed and p-values < 0.05 were considered statistically significant. Surface morphology measurements were statistically analyzed by non-parametric Mann-Whitney-*U* test and p-values < 0.05 (corrected post hoc according to Bonferroni) were considered statistically significant. In addition, quantitative tissue analysis and biomechanics were statistically evaluated by an unpaired students-*t*-test and p-values p < 0.05 (corrected post hoc according to Bonferroni) were considered statistically significant. KS normality test was used to confirm normal distribution of the dataset (p > 0.05). All statistical analyses were performed using the GraphPad Prism 5 software (GraphPad Software Inc., USA).

3. Results

3.1. Phenotype and proliferation of umbilical cord derived fibroblasts

Immunofluorescence performed on fibroblasts derived from three different patients revealed that all cell types displayed similar immunophenotypic patterns. Isolated human fibroblasts expressed myogenic markers, such as alpha smooth muscle actin and vimentin, and common fibroblast marker CD90 (Fig. 1a).

In contrast, the cells were negative for the endothelial cell surface marker CD31 excluding non-fibroblastic contamination during cell isolation procedures. In the proliferation analysis based on crystal violet staining (Fig. 1b), no significant differences in proliferation parameters were detected between the three fibroblast lines when considering cell numbers over 7 days (p < 0.05). These findings exclude potential significant inter-individual proliferation differences.

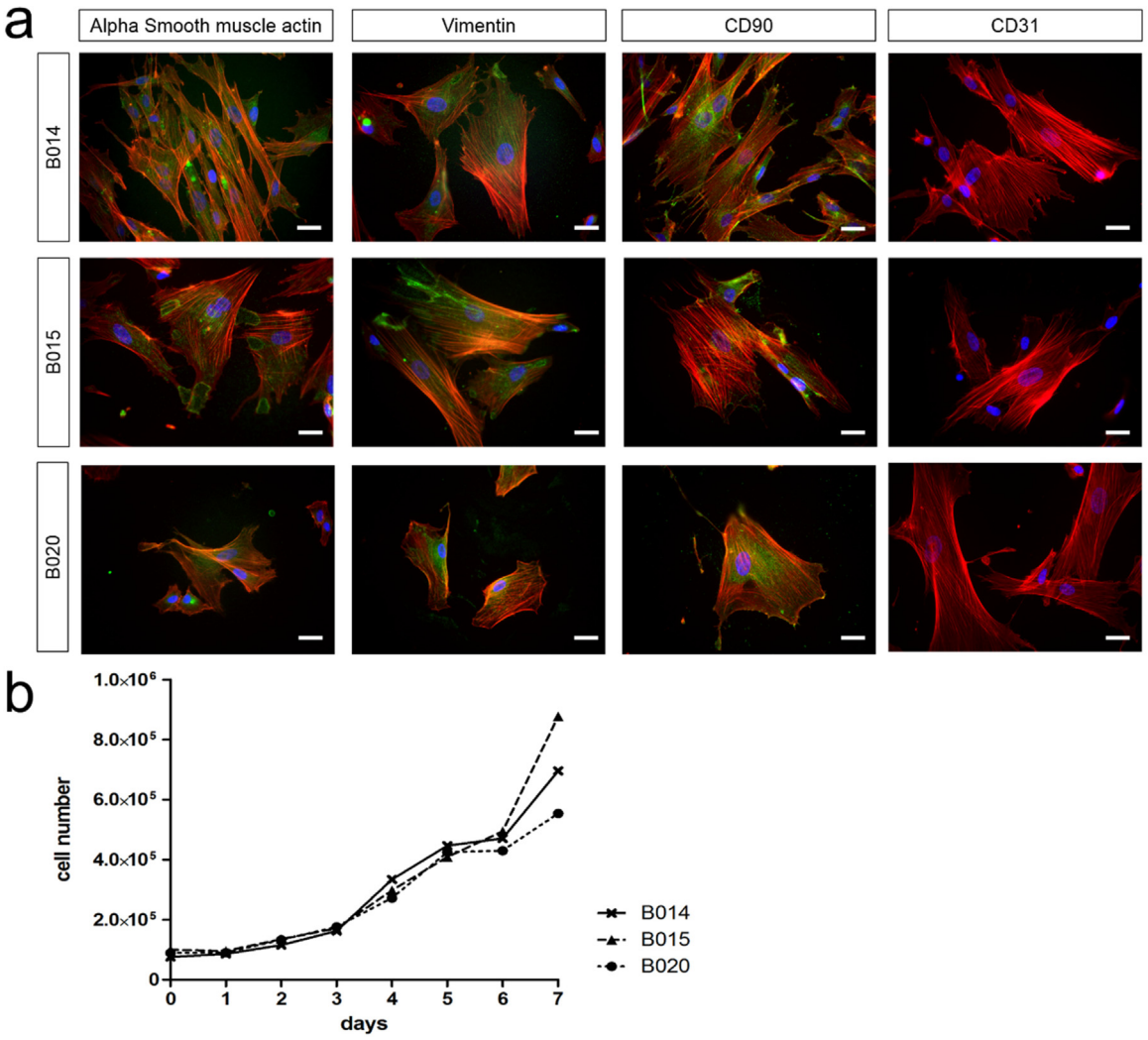

Fig. 1. Phenotypic characterization and proliferation of isolated fibroblasts. a) Immunohistochemical analyses of three different human fibroblast cell lines (B014, B015 and B020) revealed positive expression of alpha smooth muscle actin, Vimentin and CD90 (Phalloidin in red, Dapi in blue and respective antibody in green). All three markers showed a homogenous expression pattern. Fibroblasts were negative for the endothelial cell surface marker CD31. b) Cell number was determined over one week for all three cell lines using the crystal violet-based proliferation assay. No significant differences were detected. (Scale bars: 50 μm). (For interpretation of the references to colour in this figure legend, the reader is referred to the web version of this article.)

3.2. Surface morphology of biomaterials

Microstructural analysis using scanning electron microscopy (SEM) was used to analyze the fiber size and porosity of unseeded polymers before and after coating (Fig. 2a–d and f–i) (n = 4 per condition).

The PGA-PCL matrix (Fig. 2a and f) was less porous in comparison to the hybrid polymers PGA-P4HB (Fig. 2b and g), PGA-PLA (Fig. 2c and h), and PGA (Fig. 2d and i). Quantitative measurements of the porosity confirmed these differences (Fig. 2j). PGA-PCL scaffolds were significantly less porous than PGA-P4HB ($p < 0.05$) or PGA-PLA ($p < 0.05$) scaffolds. PGA-P4HB and PGA-PLA scaffolds showed a similar porosity with no significant difference ($p = 0.69$). Uncoated PGA mesh was significant more porous in comparison to PGA-P4HB ($p < 0.05$), PGA-PLA ($p < 0.05$), and PGA-PCL ($p < 0.05$). The fiber diameter was uniform among all biomaterials with no statistically significant differences between different hybrid polymer groups or uncoated PGA (Fig. 2g, $p < 0.05$) (Fig. 2e). Imaging of the surface (Fig. 2a–d) and cross section (Fig. 2f–i) display the distribution of the coating compared to PGA scaffold only. The different hybrid polymer present a similar distribution of the coating. In general, there was more coating visible on the outer scaffold regions, while in the central part of the scaffold less was detected.

3.3. Qualitative tissue analyses

Microstructural features of human fibroblast-derived TE patches were analyzed by histological staining procedures (Fig. 3) as well as polarization microscopy (Fig. 4).

H&E staining demonstrated formation of extracellular matrix (ECM) *in vitro* with high cellularity and layered tissue on the outer scaffold regions, while in the central part of the scaffold low cellularity and no significant formation of ECM were present. In order to investigate the deposition of collagen fibers Masson Trichom staining was used. In general, TE patches under dynamic conditions (Fig. 3, right column) revealed more tissue formation and ECM deposition compared to static conditions.

Importantly, all three cell lines exhibited comparable tissue formation for respective hybrid polymer conditions excluding a potential bias due to inter-individual differences. PGA-PCL-based patches showed for both culture conditions (dynamic and static) less tissue formation and high quantities of scaffold remnants in

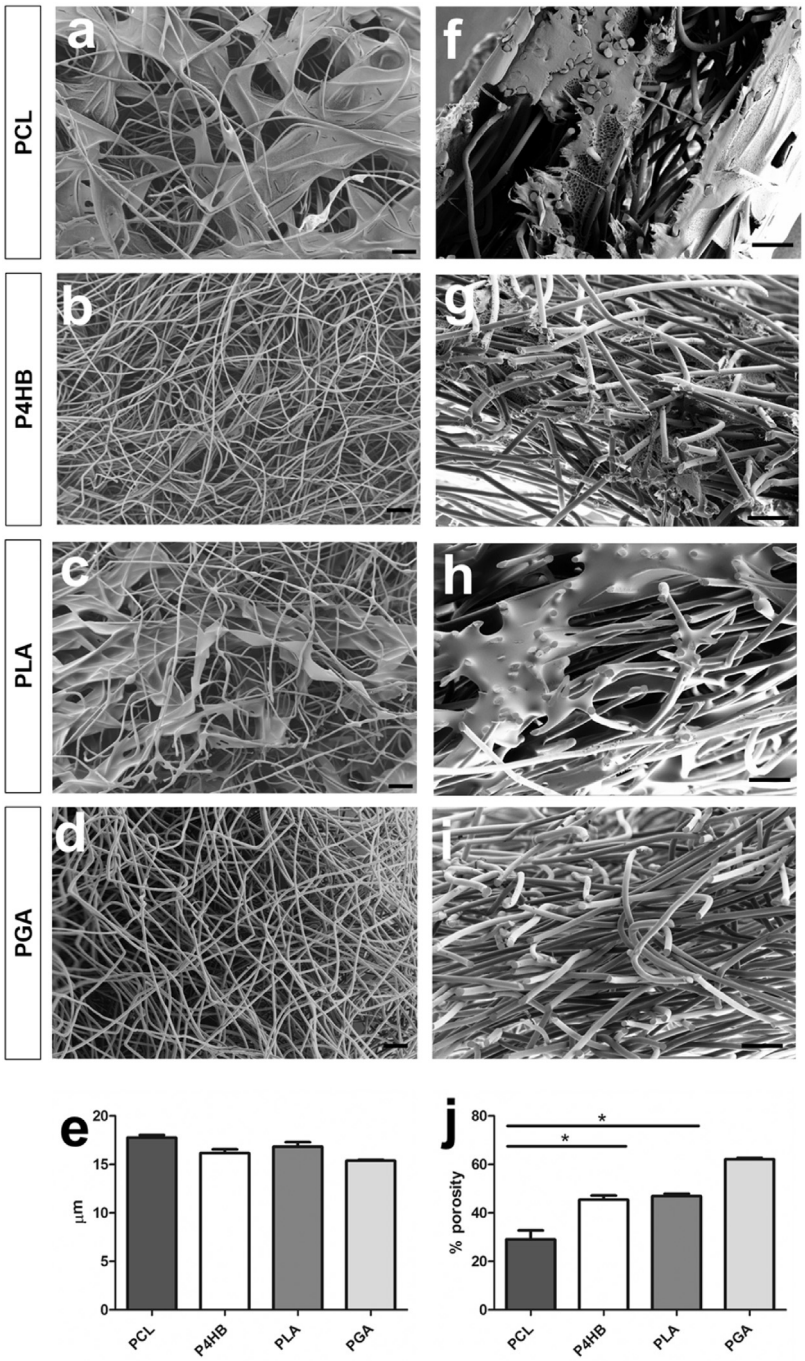

Fig. 2. Surface and intersection morphology of biomaterials. Scanning electron micrographs (SEM) show the fiber alignment and size of unseeded biomaterials. a–d) SEM of the surface f–i) SEM of the cross section e) the fiber diameter was consistent among all biomaterials. (n = 4) j) PGA-PCL was significantly less porous than PGA-P4HB or PGA-PLA. PGA-P4HB and PGA-PLA showed a similar porosity. (n = 4) (Scale bars: 100 μm).

comparison to the PGA-P4HB or PGA-PLA. In order to confirm these findings polarization microscopy was performed to further visualize different polymer components (Fig. 4).

The starter matrices showed no major remodeling in the central part of the constructs in static as well as dynamic conditions given the lack of tissue formation in this area of the constructs. PGA fibers were visible as elongated ellipses (Fig. 4, high magnification), whereas the webbings between PGA fibers represented remnants of the coating (Fig. 4, low magnification). In dynamic conditions the biomaterial was more degraded (Fig. 4d–f) when compared to the static cultures (Fig. 4a–c). In particular, the PGA-PCL starter matrix (Fig. 4b and e) showed strong preservation of the polymer components compared to PGA-P4HB (Fig. 4a and d) or PGA-PLA (Fig. 4c and f).

3.4. Quantitative tissue analysis

The composition of the ECM of the human fibroblast-derived TE constructs was biochemically analyzed using assays for HYP, GAG, and the cell number (DNA) (Fig. 5).

The expression level of DNA, GAG, and HYP is for all 3 coatings higher under dynamic conditions than under static conditions. Analyses were performed after three weeks of static or dynamic culture. In general, no significant differences were detected between

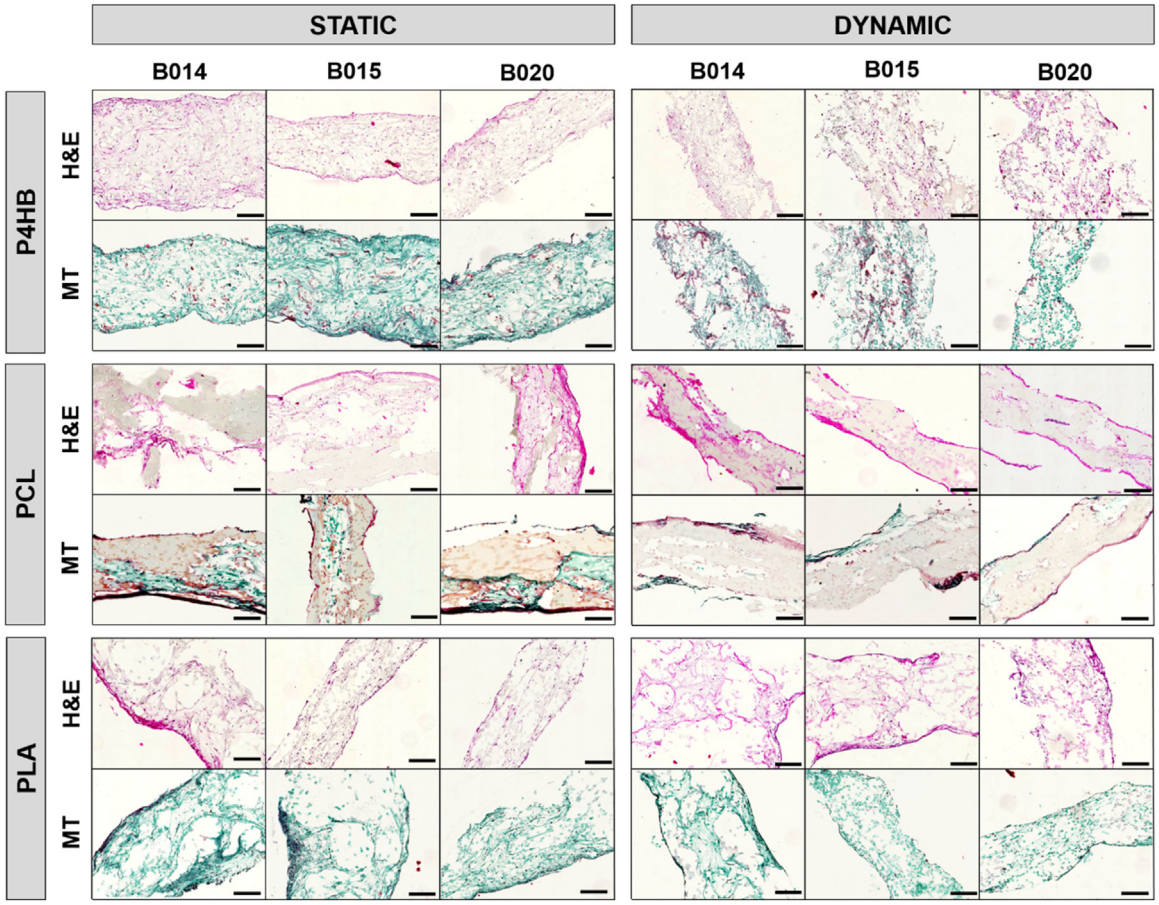

Fig. 3. Histology of tissue-engineered patches under static and dynamic conditions. Hematoxylin-eosin (H&E) staining of statically cultured tissue-engineered patches (left column) revealed cellular ingrowth with tissue formation, and some collagen fibers could be detected with Masson Trichrome staining (MT). In contrast, patches cultured under dynamic conditions (right column) demonstrated more cellular tissue formation and production of extracellular matrix elements. All three cell lines displayed similar tissue formation for respective conditions/coatings. PGA-PCL patches showed for both culture conditions less tissue formation and high quantities of scaffold remnants in comparison to PGA-P4HB or PGA-PLA. (Scale bars: 200 μm).

the three different cell lines relating to expression of HYP, GAG and DNA for respective coatings under static or dynamic conditions, indicating no inter-individual differences. In total, six TE patches per cell line and per coating condition were analyzed. PGA-P4HB showed a significantly higher expression of DNA, GAG, and HYP in comparison to PGA-PLA ($p < 0.05$) or PGA-PCL ($p < 0.05$) under static conditions suggesting a more rapid formation of ECM *in vitro*. Moreover, PGA-PLA exhibited a significantly higher expression of DNA and HYP than PGA-PCL ($p < 0.05$) under static conditions. Dynamically cultured PGA-PLA ($p < 0.05$) and PGA-P4HB ($p < 0.05$) patches expressed a significantly higher amount of DNA, GAG and HYP than PGA-PCL patches. PGA-P4HB ($p < 0.05$) also displayed a significantly higher DNA and HYP expression than PGA-PLA. In general, the expression levels of DNA, GAG and HYP were higher for all coatings under dynamic conditions compared to statically cultured patches.

3.5. Biomechanics

The material properties of the different TE patches used in this study were determined *via* uniaxial tensile tests in comparison to native ovine tissue, such as cartilage, skin and vein (Fig. 6). Stress–strain curves were obtained and Young's modulus was determined as the slope of the curve at a strain of 10%, as a measure for tissue stiffness. Contribution of tissue formation to the mechanical properties was observed in all TE patches, given a higher elasticity with culture time in comparison to unseeded control. Due to the rapid loss of mechanical integrity of the scaffold, biomechanical tests on the TE patches under dynamic conditions over time could not be performed. Overall, PGA-PLA and PGA-P4HB TE patches show similar biomechanical properties. Both conditions display tensile stress of about 0.02 MPa and strain at maximal stress of about 20%. Tensile moduli of both 0.04 MPa and 0.08 MPa were obtained, which were not significantly different ($p = 0.1479$). In case of PGA-PCL, tensile stress was 0.54 MPa, tensile strain was 8%, and having a Young's modulus of 4 MPa respectively. Generally, PGA-PCL showed a significantly higher Young's modulus, tensile strength and lower strain at maximal stress compared to PGA-PLA ($p < 0.05$) or PGA-P4HB ($p < 0.05$). For a better interpretation of the obtained results, also native ovine tissue were analyzed biomechanically. For cartilage, Young's modulus was about 35 MPa, tensile strength was 12 MPa, and strain at maximal stress was 32.5%. In addition, skin had a Young's modulus of 0.005 MPa, tensile stress of 14.5 MPa and tensile strain of 160%. Similar results were found for the vein with a Young's of 0.0054 MPa, a tensile stress of 2 MPa and tensile strain of 185%.

4. Discussion

The tissue formation produced by implanted cells is highly influenced by the scaffold onto which they are seeded. Different types of biodegradable polymers as a scaffold have been investigated for tissue regeneration, such as PGA, PLA, P4HB and PCL [8,10,20]. Therefore, the present study aimed at a systematic, multimodal comparison of three frequently used polymers for the *in vitro* engi-

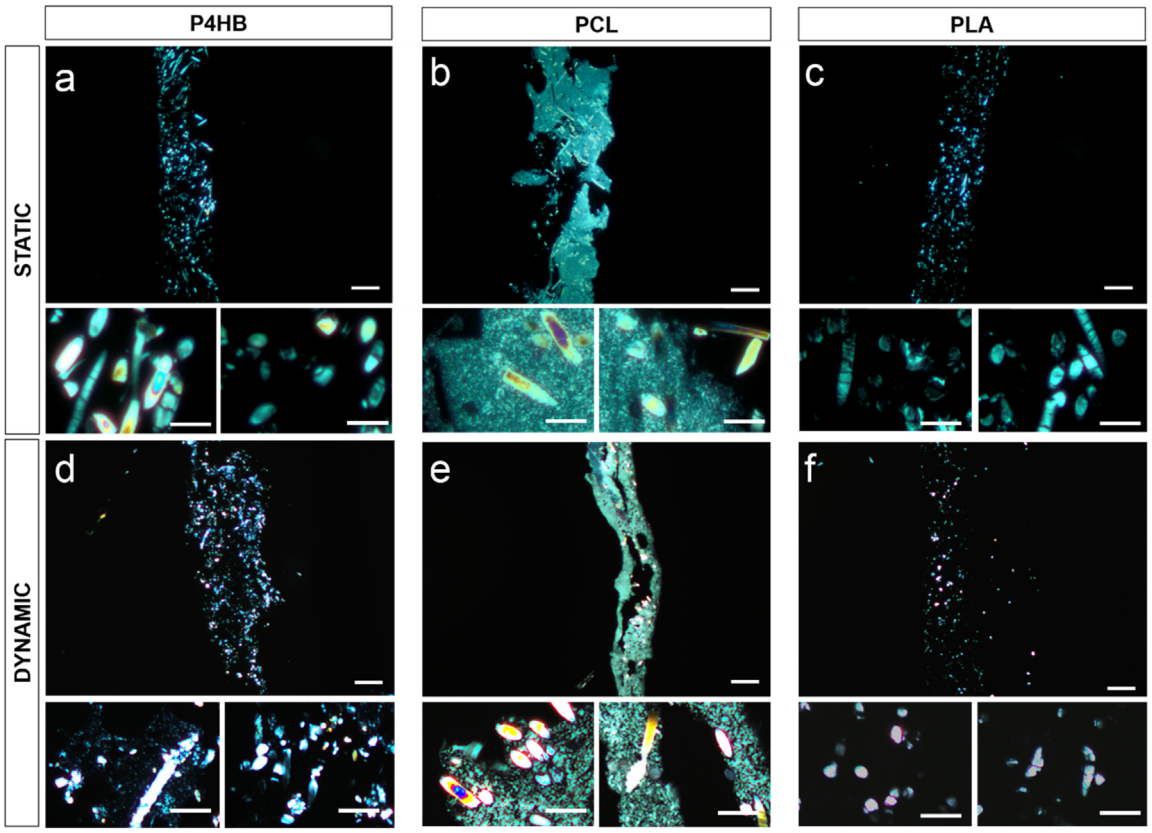

Fig. 4. Polarization microscopy of tissue-engineered patches under static and dynamic conditions. Polarization microscopy revealed the presence of the initial scaffold matrix in particular in the central part of the constructs. PGA fibers are shown as elongated ellipses (high magnification). Webbings between PGA fibers represent coating remnants (low magnification). However, in the dynamic fibroblast-based constructs the biomaterial remnants were more degraded (d–f) compared with static cultures (a–c). PGA-PCL (b and e) starter matrix showed a very strong preservation of the co-polymer when compared to PGA-P4HB (a and d) or PGA-PLA (c and f) scaffolds (scale bars: 400 μm low magnification, 100 μm high magnification).

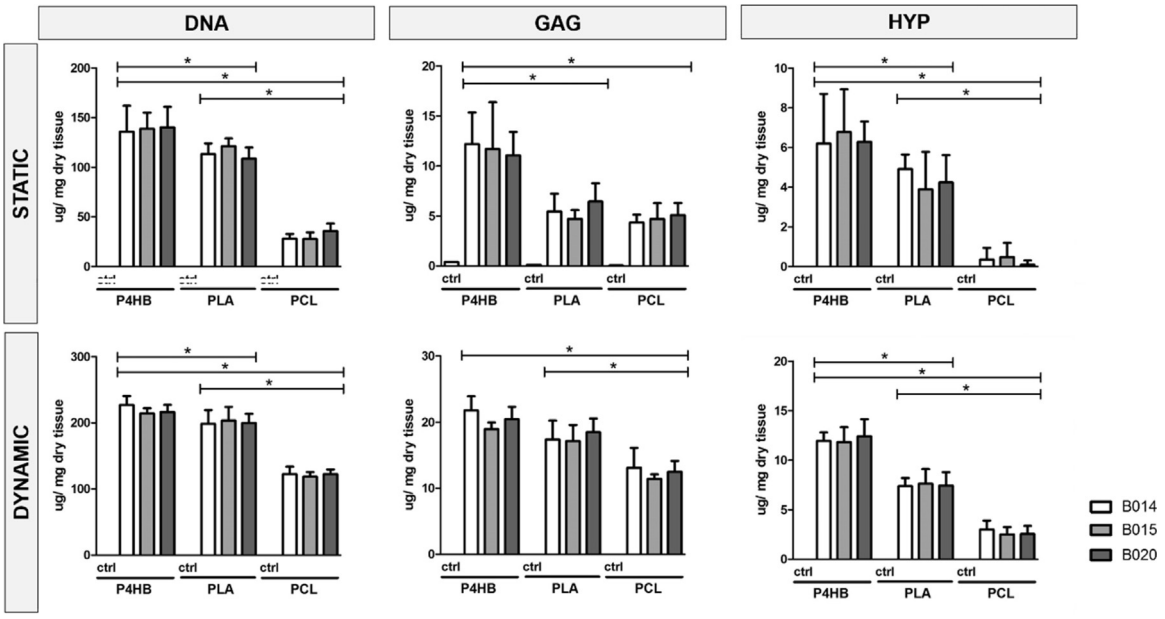

Fig. 5. Extracellular matrix analysis of tissue-engineered patches under static and dynamic conditions. Extracellular matrix analysis shows the amount of hydroxyproline (HYP), glycosaminoglycans (GAG), and the cell number (deoxyribonucleic acid, DNA) of tissue-engineered patches, which were statically or dynamically cultured (all values relative to control samples (ctrl) indicating biomaterials only). Generally, all three cell lines displayed similar amounts of HYP, GAG and DNA for respective conditions/coatings, no significant differences were detected. Overall PGA-P4HB (n = 6) showed a higher expression of DNA, GAG, and HYP in comparison to PGA-PLA (n = 6) or PGA-PCL (n = 6).

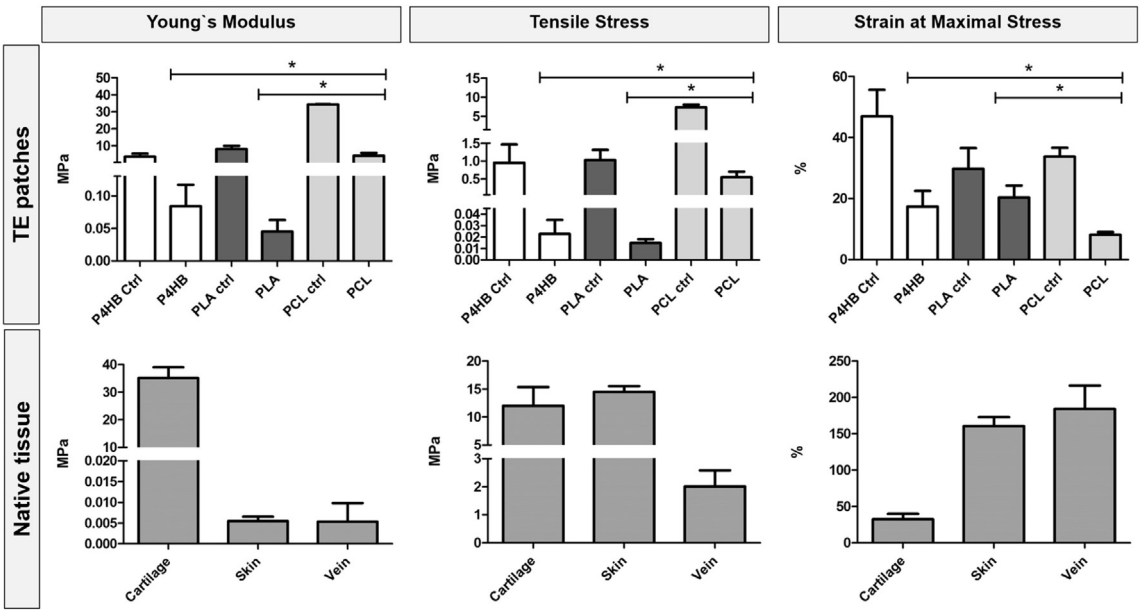

Fig. 6. Mechanical properties of tissue-engineered patches and native tissue. Stress–strain curves were obtained and Young's modulus was determined as the slope of the curve at a strain of 10%, as a measure for tissue stiffness. Control (ctrl) means biomaterials only. Generally, PGA-PCL (n = 12, 4 patches per group) showed a significant higher Young's modulus, tensile strength and lower strain at maximal stress compared to PGA-PLA (n = 12) or PGA-P4HB (n = 12). As a comparison cartilage, skin and vein samples (n = 4) were also tested.

neering of extracellular matrix under static as well as dynamic conditions.

So far, most biomaterials do not completely mimic physiological microenvironment and can therefore not enable native like cellular interaction and behavior [15]. Blending two polymers has gathered growing interest for constructing native-like tissues [15]. Thus, patches were cut from PGA meshes and coated with same concentrations of either P4HB, PLA, or PCL. In addition, to mimic the native tissue and serving as an artificial environment, the structure and surface morphology of the scaffolds have to meet general requirements: (I) pores to ensure cell growth and nutrients/metabolic waste transport; (II) three-dimensional architecture; (III) suitable mechanical properties depending on the native tissue to be replaced; (IV) suitable surface chemistry; (V) biodegradation and bioresorbability [35]. Moreover, pore size affects cell binding, migration depth of cellular in-growth, cell morphology, and phenotypic expression [36].

For this reason, we performed SEM to analyze the ultra-structure of the unseeded scaffold. SEM confirmed the uniform fiber diameters of the coated PGA matrix. In contrast, PGA-PCL scaffolds were significantly less porous than PGA-P4HB or PGA-PLA scaffolds. PGA-P4HB and PGA-PLA scaffolds showed a similar porosity. These findings already suggested a potential improved cell infiltration and consequent tissue formation for PGA-P4HB and PGA-PLA in comparison to PGA-PCL. For example, porosity of the scaffold plays an important role in bone and cartilage regeneration [37,38]. Interestingly, lower porosity enhances osteogenesis by suppressing cell proliferation and forcing cell aggregation *in vitro* [38]. In contrast, higher porosity and larger pore size lead to greater bone ingrowths to the scaffold but diminish the mechanical properties *in vivo* [38]. However, one has to take into account that for comparative issues the concentrations of P4HB, PLA, and PCL were consistent and could be further adapted for specific requirements.

Hence, microstructural features of human fibroblast-derived TE patches were analyzed by histological stainings as well as polarization microscopy. In general, tissue engineered patches under dynamic conditions represented a more extensive tissue formation and ECM deposition. Tang et al. also showed an enhanced cell proliferation under dynamic three-dimensional (3D) culture compared with conventional static two-dimensional (2D) and 3D cell culture conditions [39]. In addition, high-throughput microarray analysis showed that gene expressions of dynamic 3D system displayed significant differences in cell proliferation and differentiation compared with static-2D conditions [39]. Nonetheless, PGA-PCL based patches displayed less tissue formation and higher quantities of scaffold remnants in comparison to the PGA-P4HB or PGA-PLA under static as well as under dynamic conditions.

In general, dynamic conditions enhanced the degradation of biomaterial in comparison to static conditions. In particular, less PGA fibers were detectable after 3 weeks of culture in comparison to the webbings between the PGA fibers, especially PGA-PCL showed particularly strong preservation of the polymer components. Different studies have proven that PGA degrades faster than P4HB, PLA and PCL [40,41]. In addition, production conditions of synthetic polymers can be tightly controlled, hence making mechanical and physical properties well defined and predictable. For instance, the time to complete degradation and resorption of P4HB varies with size and processing, *i.e.*, the orientation of the polymer fibers. In general, complete resorption of P4HB occurs between 12 and 18 months *in vivo* [40]. The characteristics of PLA are highly affected by the stereo-isomeric L/D ratio of lactate units [8]. Generally, an increased stereo-isomeric ratio decreases the crystallinity, whereby the degradation is enhanced. For example, degradation of PLA is faster than PDLA due to the lower crystallinity of PLA [8]. PLA and PCL degradation takes longer than 24 months *in vivo* [41]. In contrast, PGA is degraded within 4–6 months *in vivo* [15,16]. The composition of the ECM of human fibroblast-derived TE constructs was analyzed and PGA-P4HB showed a significantly higher expression of DNA, GAG, and HYP in comparison to PGA-PLA or PGA-PCL under static conditions suggesting a more rapid formation of ECM *in vitro*. The interactions between cells and ECM are essential in cell attraction, cell differentiation and wound healing [42]. Dynamically cultured PGA-PLA and PGA-P4HB patches expressed a significantly higher amount of DNA, GAG and HYP than PGA-PCL patches. The general expression levels of DNA, GAG and HYP were higher for all coatings under dynamic conditions compared to statically cultured

patches. These findings confirm and underline the findings in histology. It is proven that mechanobiological interactions between cells and scaffolds can crucially influence cell behavior [43–45]. For example, the mechanobiologic regulation of cartilage matrix biosynthesis was successfully exploited by the application of cyclic compression to constructs formed by encapsulating primary bovine chondrocytes in agarose hydrogels [45,46]. By 28 days, determined improvements in the compressive stiffness were observed in groups that had been exposed to mechanical loading compared with free swelling controls [46]. Even though relations between these forces and cell responses are exhibited, elucidation of the mechanotransduction pathways is far from revealed. The transduction of external forces to signaling pathways involves intracellular forces and associated molecular deformations, such as gap junctions on the cell membrane, the cytoskeleton, and DNA [44,45].

Importantly, a balance between the rate of scaffold degradation and tissue formation is crucial for maintaining mechanical integrity of the replaced tissues [47]. The biodegradable scaffold should have sufficient mechanical properties (such as strength and stiffness) approximating those of the host tissue until the biodegradable scaffold matrix is substituted by the new tissue [47]. The material properties of different TE patches used in this study were determined *via* uniaxial tensile tests. In addition, we compared these values with native ovine cartilage, skin and vein tissue. Contribution of tissue formation to the mechanical properties was observed in all TE patches, as samples became less stiff with culture time in comparison to unseeded controls. Overall, PGA-PLA and PGA-P4HB TE patches show similar biomechanical properties. Generally, PGA-PCL showed a significant higher Young's modulus, tensile strength and lower strain at maximal stress compared to PGA-PLA or PGA-P4HB. Meaning that on one hand PGA-PCL is stiffer and on the other hand is more robust than PGA-P4HB and PGA-PLA. Notably, in contrast to PGA-PCL, PGA-P4HB and PGA-PLA are more ductile and flexible. The values are still not in the range of native tissue but this may rely on the polymer remnants and the incomplete tissue formation *in vitro*. However, as with many polymers, the mechanical properties of the material depend not only on the basal material, but also on its processing history [40].

5. Conclusion

Biodegradable synthetic polymers are an interesting raw material for scaffold fabrication and have been intensively investigated for TE. As the scaffold plays a crucial role in the successful design of TE constructs, the choice of material directly influences the outcome. Our study may allow for a specific selection of a certain polymer starter matrices aiming at specific tissue properties of bioengineered materials *in vitro*. In general, we showed that PGA-P4HB coating display better tissue formation and a significant higher expression level of DNA, GAG and HYP in comparison to PGA-PLA and PGA-PCL. However, PGA-PCL is under biomechanical conditions more robust than PGA-P4HB and PGA-PLA.

Future studies are required to evaluate, which combination under which conditions allow for the best tissue formation and native-like biomechanical properties.

Author disclosure statement

The authors declare no competing or conflicting financial interests.

Acknowledgments

The authors would like to thank Nicole Gampp, Ursula Steckholzer, Nicole Gross and Ulrich Bleul for their technical help and assistance. Furthermore, we would like to thank Kirill Feldmann for the biomechanical advice and assistance. The research leading to these results has received funding from the Swiss National Science Foundation (Project 310030_143992), Forschungskredit Candoc of the University of Zurich, Forschungskredit Postdoc of the University of Zurich, the Foundation for Research in Science and the Humanities at the University of Zurich and the Alfred and Anneliese Sutter-Stöttner-Foundation.

References

[1] R. Langer, J.P. Vacanti, Tissue engineering, Science 260 (5110) (1993) 920–926.
[2] P. Yuan, et al., Design, development and clinical validation of computer-aided surgical simulation system for streamlined orthognathic surgical planning, Int. J. Comput. Assist. Radiol. Surg. 12 (2017) 1–15.
[3] Q. Li, L. Ma, C.Y. Gao, Biomaterials for in situ tissue regeneration: development and perspectives, J. Mater. Chem. B 3 (46) (2015) 8921–8938.
[4] B. Hu, C. Ye, C.Y. Gao, Synthesis and characterization of biodegradable polyurethanes with unsaturated carbon bonds based on poly(propylene fumarate), J. Appl. Polym. Sci. 132 (24) (2015).
[5] X.P. Bi, et al., A functional polyester carrying free hydroxyl groups promotes the mineralization of osteoblast and human mesenchymal stem cell extracellular matrix, Acta Biomater. 10 (6) (2014) 2814–2823.
[6] W.Y. Cai, et al., Carboxyl-ebselen-based layer-by-layer films as potential antithrombotic and antimicrobial coatings, Biomaterials 32 (31) (2011) 7774–7784.
[7] A. Philipp, et al., Functional modification of amide-crosslinked oligoethylenimine for improved siRNA delivery, React. Funct. Polym. 71 (3) (2011) 288–293.
[8] P.E. Dijkman, et al., Polymeric starter matrices for cardiovascular tissue engineering, in: Encyclopedia of Biomedical Polymers and Polymeric Biomaterials, CRC Press, 2015, pp. 1–25.
[9] P. Sensharma, et al., Biomaterials and cells for neural tissue engineering: current choices, Mater. Sci. Eng. C Mater. Biol. Appl. 77 (2017) 1302–1315.
[10] G.Q. Chen, Q. Wu, The application of polyhydroxyalkanoates as tissue engineering materials, Biomaterials 26 (33) (2005) 6565–6578.
[11] P. Nooeaid, et al., Osteochondral tissue engineering: scaffolds, stem cells and applications, J. Cell. Mol. Med. 16 (10) (2012) 2247–2270.
[12] B. Rentsch, et al., Embroidered and surface coated polycaprolactone-co-lactide scaffolds: a potential graft for bone tissue engineering, Biomatter 2 (3) (2012) 158–165.
[13] A. Mol, et al., Autologous human tissue-engineered heart valves: prospects for systemic application, Circulation 114 (Suppl. 1) (2006) I152–8.
[14] B. Weber, et al., Injectable living marrow stromal cell-based autologous tissue engineered heart valves: first experiences with a one-step intervention in primates, Eur. Heart J. 32 (22) (2011) 2830–2840.
[15] A. Asti, L. Gioglio, Natural and synthetic biodegradable polymers: different scaffolds for cell expansion and tissue formation, Int. J. Artif. Organs 37 (3) (2014) 187–205.
[16] A.S. Dunn, P.G. Campbell, K.G. Marra, The influence of polymer blend composition on the degradation of polymer/hydroxyapatite biomaterials, J. Mater. Sci. Mater. Med. 12 (8) (2001) 673–677.
[17] T. Sugiura, et al., Tropoelastin inhibits intimal hyperplasia of mouse bioresorbable arterial vascular grafts, Circulation 134 (2016).
[18] Q. Wu, Y. Wang, G.Q. Chen, Medical application of microbial biopolyesters polyhydroxyalkanoates, Artif. Cells Blood Substit. Immobil. Biotechnol. 37 (1) (2009) 1–12.
[19] P. Saini, M. Arora, M.N. Kumar, Poly(lactic acid) blends in biomedical applications, Adv. Drug Deliv. Rev. 107 (2016) 47–59.
[20] I. Engelberg, J. Kohn, Physico-mechanical properties of degradable polymers used in medical applications: a comparative study, Biomaterials 12 (3) (1991) 292–304.
[21] F. Couet, N. Rajan, D. Mantovani, Macromolecular biomaterials for scaffold-based vascular tissue engineering, Macromol. Biosci. 7 (5) (2007) 701–718.
[22] H. Li, R. Du, J. Chang, Fabrication, characterization, and in vitro degradation of composite scaffolds based on PHBV and bioactive glass, J. Biomater. Appl. 20 (2) (2005) 137–155.
[23] T. Shinoka, et al., Creation of viable pulmonary artery autografts through tissue engineering, J. Thorac. Cardiovasc. Surg. 115 (3) (1998) 545–546, discussion 545–6.
[24] X. Wu, et al., Tissue-engineered microvessels on three-dimensional biodegradable scaffolds using human endothelial progenitor cells, Am. J. Physiol. Heart Circ. Physiol. 287 (2) (2004) H480–7.
[25] G. Matsumura, et al., Long-term results of cell-free biodegradable scaffolds for in situ tissue-engineering vasculature: in a canine inferior vena cava model, PLoS One 7 (4) (2012) e35760.
[26] M. Watanabe, et al., Tissue-engineered vascular autograft: inferior vena cava replacement in a dog model, Tissue Eng. 7 (4) (2001) 429–439.
[27] D. Schmidt, U.A. Stock, S.P. Hoerstrup, Tissue engineering of heart valves using decellularized xenogeneic or polymeric starter matrices, Philos. Trans. R. Soc. Lond. B Biol. Sci. 362 (1484) (2007) 1505–1512.

[28] S.P. Hoerstrup, et al., Functional living trileaflet heart valves grown in vitro, Circulation 102 (19 Suppl 3) (2000), III44-9.
[29] B. Weber, et al., Off-the-shelf human decellularized tissue-engineered heart valves in a non-human primate model, Biomaterials 34 (30) (2013) 7269–7280.
[30] S.R. Son, et al., In vitro and in vivo evaluation of electrospun PCL/PMMA fibrous scaffolds for bone regeneration, Sci. Technol. Adv. Mater. 14 (1) (2013).
[31] L.V. Thomas, V. Lekshmi, P.D. Nair, Tissue engineered vascular grafts–preclinical aspects, Int. J. Cardiol. 167 (4) (2013) 1091–1100.
[32] S.P. Hoerstrup, et al., Living, autologous pulmonary artery conduits tissue engineered from human umbilical cord cells, Ann. Thorac. Surg. 74 (1) (2002) 46–52, discussion 52.
[33] R.W. Farndale, D.J. Buttle, A.J. Barrett, Improved quantitation and discrimination of sulphated glycosaminoglycans by use of dimethylmethylene blue, Biochim. Biophys. Acta 883 (2) (1986) 173–177.
[34] G. Huszar, J. Maiocco, F. Naftolin, Monitoring of collagen and collagen fragments in chromatography of protein mixtures, Anal. Biochem. 105 (2) (1980) 424–429.
[35] L. Olah, L. Borbas, Properties of calcium carbonate-containing composite scaffolds, Acta Bioeng. Biomech. 10 (1) (2008) 61–66.
[36] F.J. O'Brien, et al., The effect of pore size on cell adhesion in collagen-GAG scaffolds, Biomaterials 26 (4) (2005) 433–441.
[37] S.R. Frenkel, et al., Regeneration of articular cartilage – evaluation of osteochondral defect repair in the rabbit using multiphasic implants, Osteoarthr. Cartil. 13 (9) (2005) 798–807.
[38] V. Karageorgiou, D. Kaplan, Porosity of 3D biomaterial scaffolds and osteogenesis, Biomaterials 26 (27) (2005) 5474–5491.
[39] Y. Tang, et al., The combination of three-dimensional and rotary cell culture system promotes the proliferation and maintains the differentiation potential of rat BMSCs, Sci. Rep. 7 (1) (2017) 192.
[40] S.F. Williams, S. Rizk, D.P. Martin, Poly-4-hydroxybutyrate (P4HB): a new generation of resorbable medical devices for tissue repair and regeneration, Biomed. Tech. (Berl.) 58 (5) (2013) 439–452.
[41] P.A. Gunatillake, R. Adhikari, Biodegradable synthetic polymers for tissue engineering, Eur. Cell Mater. 5 (2003) 1–16, discussion 16.
[42] A. Phadke, C.W. Chang, S. Varghese, Functional biomaterials for controlling stem cell differentiation, Biomater. Stem Cell Niche 2 (2010) 19–44.
[43] P.A. Janmey, C.A. McCulloch, Cell mechanics: integrating cell responses to mechanical stimuli, Annu. Rev. Biomed. Eng. 9 (2007) 1–34.
[44] F. Guilak, et al., Biomechanics and mechanobiology in functional tissue engineering, J. Biomech. 47 (9) (2014) 1933–1940.
[45] D.L. Butler, et al., The impact of biomechanics in tissue engineering and regenerative medicine, Tissue Eng. Part B Rev. 15 (4) (2009) 477–484.
[46] R.L. Mauck, et al., Functional tissue engineering of articular cartilage through dynamic loading of chondrocyte-seeded agarose gels, J. Biomech. Eng. 122 (3) (2000) 252–260.
[47] H.J. Chung, T.G. Park, Surface engineered and drug releasing pre-fabricated scaffolds for tissue engineering, Adv. Drug Deliv. Rev. 59 (4–5) (2007) 249–262.